

Characterization of the performance of commercial Ni/MH batteries

Gowri S. Nagarajan, J.W. Van Zee *

Department of Chemical Engineering, University of South Carolina, Columbia, SC 29208, USA

Received 24 March 1997; accepted 18 April 1997

Abstract

An experimental study is presented for the characterization of commercially available Ni/MH batteries. An experimental study of AA-size cells from Matsushita, Sanyo, and Toshiba was performed to determine the charge and discharge behavior at different rates. The self-discharge characteristics, the cycle-life characteristics, and the effect of temperature on the charge and discharge characteristics are also reported at various rates. Apart from the performance study, a couple of cells from each manufacturer were disassembled to gain insight into the design of the cell and to characterize the separator. The characterization results show that although the three cells were identical in nominal capacity, weight and size, their performance greatly differed in terms of charge and discharge behavior, high rate discharge capabilities, self-discharge losses, charging efficiency, and cycle life. © 1998 Elsevier Science S.A.

Keywords: Characterization; Ni/MH batteries; Performance; Experimental

1. Introduction

Ni/MH rechargeable batteries are gaining popularity over the Ni/Cd battery [1] with increasing environmental concerns about cadmium, the toxic component of the battery. With increasing sophistication in the electronic products and reductions in size and weight, the power sources are expected to deliver increasingly higher levels of weight and volume energy densities. Ni/MH batteries offer a distinct advantage on a cost versus performance basis over other advanced battery systems. Recently, several automotive manufacturers have successfully demonstrated electric vehicles with Ni/MH batteries as the power source. Thus, the Ni/MH battery appears to be a practical power source for the near future for various high performance applications. Although there is an increasing interest in this battery system, data which compares existing commercial batteries has not been reported. This paper reports these comparisons with the premise that improvements in the Ni/MH battery system requires familiarity with the characteristics of state-of-art commercial batteries.

Characterization of commercially available cells offers an excellent way to understand the current stage in the development of these batteries. It provides opportunities to distinguish performance differences that might exist be-

tween these batteries. It also helps explore components of the battery which might need improvement. Finally, the characterization study could also generate data for mathematical models of this battery system. The objectives of this paper are to illustrate the differences in the performance of the batteries obtained from different manufacturers and establish the possible reasons for these differences based on the fundamentals of battery design.

The AA cells studied here were manufactured by Toshiba, Matsushita, and Sanyo and they have similar appearance in terms of physical dimensions and weight as shown in Table 1. Note that, although nominal capacity refers to the capacity that should be obtained on slow discharge, the measured capacities of the cells at $C/5$ discharge rates¹ differed from their nominal capacities. In the case of the Sanyo cells, the difference was significant, but the standard deviation is based on a sample size of only six cells and this deviation is much smaller than the 36 or 45 mAh shown for the other manufacturers.

2. Cell construction analysis

The cells were first initially conditioned at room temperature for a few cycles to stabilize their discharge capac-

* Corresponding author. Tel.: +1-803 777 41 81; Fax: +1-803-777 82 65; e-mail: vanzee@engr.sc.edu

¹ Here we define the charge rate of 1C equals 1.2 A for Toshiba and Matsushita cells and equal to 1.25 A for Sanyo cells.

Table 1

Basic information on the cells used for the study (measured capacity corresponds to the time required for the cell to reach 1.0 V)

Manufacturer	Nominal capacity (mAh)	Measured capacity at $C/5$ discharge (mAh)	Model	Number of cells used	Weight (g)	Capacity at 3C discharge ^a (%)	Residual capacity after 30 days in 45°C ^a (%)
Toshiba	1200	1220 ± 36	TH-3M 2P	6	25.16	80	35
Matsushita	1200	1191 ± 45	RP-BP-120HD-K	8	25.72	87	60
Sanyo	1250	1189 ± 20	HR-AAU	6	25.63	80	N.A.

^aIndicates product literature as source.

Table 2

Charging procedure for the cells used in the study

Manufacturer	Slow charging procedure	Fast charging procedure	Suggested charge input (% of rated capacity)
Toshiba	0.1C for 15 h	1C for 1.5 h	150
Matsushita	0.1C for 12 h	1C for 1.2 h	120
Sanyo	0.1C for 16 h	1C for 1.2 h	120

ities. This was done by choosing a slow charge/discharge protocol and the capacities attained a constant value after typically five to ten cycles. The procedure used for charging is shown in Table 2. After the conditioning step, one or two cells from each manufacturer were dissected to obtain information on the overall design and the physical characteristics of the electrode materials and the separator. Fig. 1 shows the overall cell construction of a typical AA cell. The spirally wound (often referred to as the jelly roll) negative-electrode/separator/positive-electrode assembly is held tightly inside the can so the electrodes are under compressive force. The Toshiba and Matsushita cells had negative electrodes that faced the can directly. The Sanyo cells, on the other hand, had an extra length of the separator wrapped around the negative electrode and held the jelly roll together by means of an adhesive. The Matsushita and the Toshiba cells had negative electrodes that were crimped at the top of the jelly roll to hold the roll tight after the winding of the electrodes. The positive

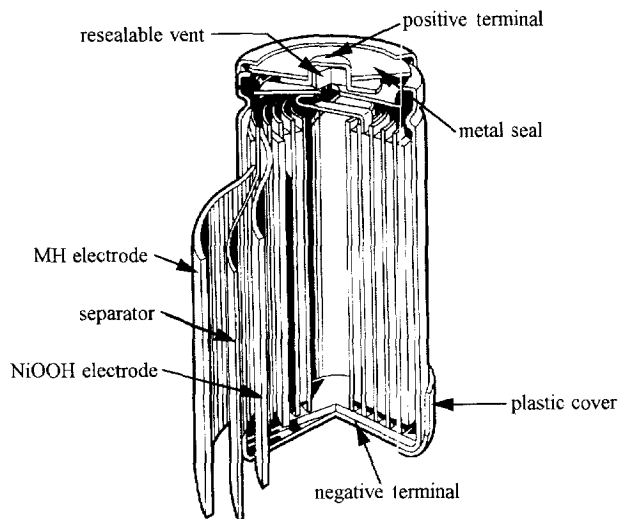


Fig. 1. Schematic of the overall construction of a typical AA cell.

electrodes had their current collectors in the form of a fine metal mesh and the tab from the center of the electrode was spot welded to the top of the can. All of the negative electrodes had a thin perforated metal foil (~5 mils in thickness) which served as the current collector and the metal hydride paste was coated uniformly on this foil. A perforated metal disc was welded to the bottom of the spirally wound metal foil and this was in turn spot welded to the bottom of the can. It was observed that the positive electrodes had developed a lot of cracks which possibly were introduced during the winding process during assembly. On the other hand, the negative electrodes had superior mechanical integrity. The disassembling of the cells gave information on the dimensions of the electrodes, the separator (see Table 3, discussed below), and the safety design incorporated in the battery.

All the cells used a resealable vent as a safety design to prevent excessive build of pressure. The vent consists of a four-piece assembly at the top of the cell placed just above the positive electrode current collector. This has a bottom plate with a small hole (diameter: 1.5 mm) at the center. This plate is slightly raised on the sides and has four small vents to release any excess pressure. The hole is covered on the top by a neoprene disc with a metal backing. A metallic spring sits on this backing and is followed by a metal cover which crimps back onto the bottom plate. Thus, when there is any excess pressure, the neoprene disc is pushed back aided by the spring on its back and the gas escapes through the side vents present on the sides of the bottom plate. It is interesting to note, however, that none of the cells had a PTC (positive temperature coefficient) device, which is the primary safety device in the lithium-ion cells used to stop the current when the cell heats up excessively [2].

Table 3 shows the physical characteristics of the electrodes. It can be seen that there is little difference between the electrodes used by the manufacturers. However, it is interesting to note that the Sanyo electrodes were thinner

Table 3
Physical characteristics of the electrodes

Brand	Positive electrode area ($L \times W$) (cm^2)	Negative electrode area ($L \times W$) (cm^2)	Active cell area (cm^2)	Positive electrode thickness (mils)	Negative electrode thickness (mils)	Negative electrode weight (g)	Positive electrode weight (g)	Positive electrode density (g/cm^3)	Negative electrode density (g/cm^3)
Toshiba	29.0	43.7	54.4	34.0	19.5	10.91	7.38	2.94	5.03
Matsushita	30.8	43.2	58.0	32.7	18.9	10.22	7.60	2.97	4.9
Sanyo	34.7	46.9	63.8	29.5	17.7	10.02	8.08	3.02	4.73

and had greater surface areas than the other two designs. The thicknesses are reported in the conventional thousands of an inch (mils) rather than cm. Table 3 shows that the positive electrode weight of the Sanyo was about 10% larger than the Toshiba. A calculation of the electrode density based on either the active area or the actual area indicates that the Sanyo positive material is most dense and the negative material is least dense of the three. The differences in thickness appear to contradict the poor high rate performance of the Sanyo cells. That is, for two electrodes with comparable weights, one expects more of the thinner electrode to be used at the same voltage with a high rate discharge because the reaction will occur at the front of the electrode.

2.1. Distribution of the mass in an AA cell

Fig. 2 shows the distribution of mass in a Toshiba Ni/MH cell. The mass distribution was very similar to the Sanyo and Matsushita cells and Table 1 shows that the average overall weight of the various cells are very similar. It can be seen that about 50% of the cell mass resides in the metal hydride electrode and this indicates that better

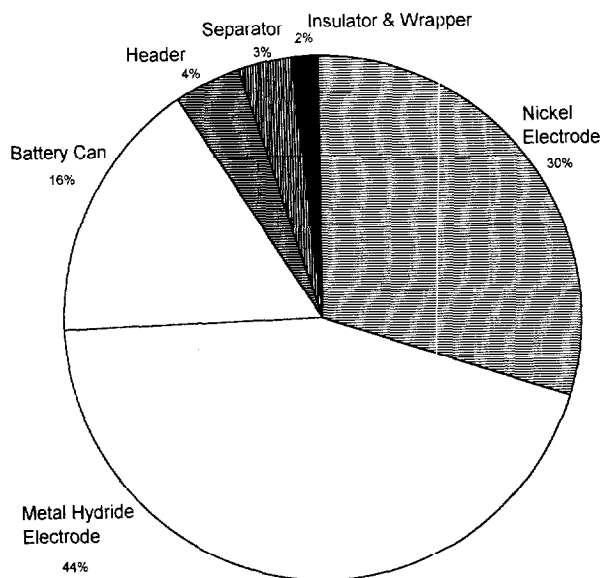


Fig. 2. Schematic of the mass distribution in the AA-size Ni/MH cell. (Note that the battery can carries a significant amount of the overall weight.) The header which includes the safety mechanism, the separator, and the insulators contribute to only 9% of the overall weight.

alloys in terms of mAh/g could certainly increase the energy density of these cells. The battery can contributes 16% of the overall weight of the battery and thus new lightweight materials for cans that could withstand the same pressure as steel could offer tremendous increase in the energy density of these cells. The other components like the header, separator, outer wrapper, and the insulators contribute only 9% to the overall weight and it seems that there is little opportunity for any reduction in their overall weight.

2.2. Separator analysis

The separators obtained by dissection from the cells were analyzed by differential scanning calorimetry (DSC) to determine the material components. That is, in all of the three cells some portion of the separator was not contaminated by the electrode material and a small piece from this portion was used for the DSC analysis. The Toshiba and the Matsushita cells were constructed so that the negative electrode was in direct contact with the can. The Sanyo cells had an extra wrap of the separator wound around the negative electrode. The three separators were similar in thickness (~ 6 mils). The separator in the Toshiba cells was identified to contain both polyethylene (PE) and polypropylene (PP) by the two endothermic peak temperatures at 130 and 170 °C, the melting points of PE and PP, respectively. The Sanyo and the Matsushita separators were identified as non-woven fabrics fabricated from conventional polyamide. Recently, Matsushita reported [3] an improved separator using sulfonated PP which has been subsequently used in their products.

3. Performance characterization

The characterization experiments were performed with a MACCOR Series 2000 battery cycler equipped with computer interface board to determine the temperature of the AA cells. Thermocouples (K-type) were used on the cells and the cycler was calibrated to generate data in °C directly. Each of the characterization studies had at least two cells. In general, the Matsushita cells had minimum variability in their behavior and the Sanyo cells exhibited the most variability. The cells were charged according to the rapid charging protocol given in Table 2 for all the

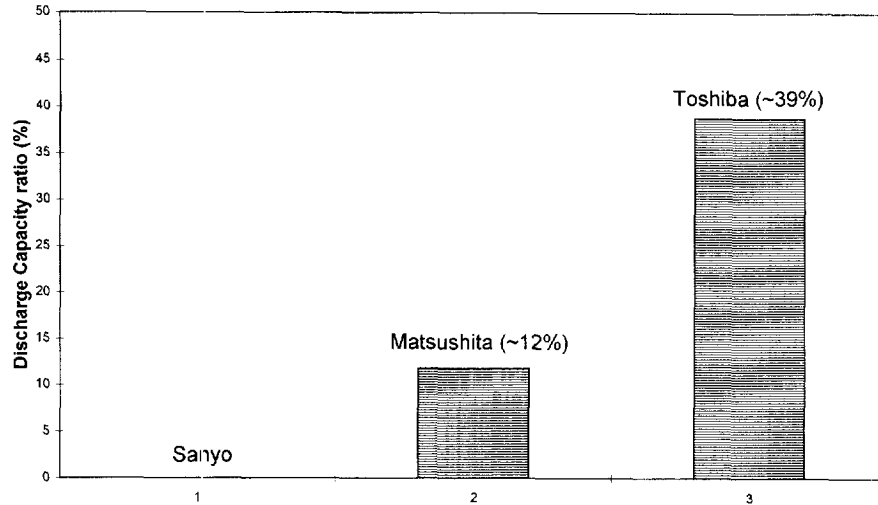


Fig. 3. Self discharge characteristics of the cells after fast charging at 1C rate and storing them at 45 °C for 30 days. The discharge was performed at a 0.2C rate. It can be seen that the Sanyo cells discharged completely during this period of time.

tests unless otherwise specified. During the tests, the temperature increased to almost 55 °C at the end of charge and the cells were immediately discharged. Thus the data contain some effect of temperature transients but no significant difference in the discharge capacity was found when the discharge began with an hour of rest after charging. The temperature of the battery decreased to room temperature during hour of rest. For the cycle-life tests, the rest period of 1 h was used between the charge and discharge experiments.

3.1. Self-discharge characteristics

Self-discharge is the loss of capacity of a fully charged cell while standing at open circuit. It is caused by the slow decomposition of both the positive and the negative electrodes due to their intrinsic instability and also due to reaction of any hydrogen in the cell with the nickel electrode. Four cells from each manufacturer were used for this study. The cells were charged according to the fast charging procedure given in Table 2 and then stored at 45 °C for a period of 30 days. High temperature was chosen because the rate of self-discharge is reported to increase with increase in temperature, thus possibly providing a clear difference between each of these cells. The discharge capacity was measured after the 30 days period using a slow discharge rate (C/5).

The results are shown in Fig. 3 where the capacity ratio is defined to be the measured capacity after the 30-day storage divided by the measured capacity immediately after charging. Fig. 3 shows that there was a significant difference in the capacity retained by the cells and these results were much lower than the data in Table 1 shown in their respective product literature. All of the Sanyo cells experienced complete self-discharge during the storage period. On the other hand, Toshiba cells were the only

ones to show similar behavior to that reported in their product literature. Since the Sanyo and the Matsushita cells used the conventional polyamide separator, the capacity retention in these cells may be poor due to the shuttle reaction of the ammonia and amine which expedites self-discharge [3].

3.2. Charge efficiency

Charge efficiency is defined as the proportion of capacity input to a cell which is subsequently available on discharge. Experiments were conducted using the fast charging procedure of Table 2. Fig. 4 shows the charge efficiency comparison for the Matsushita and Toshiba cells. The Sanyo cells exhibited similar behavior to the Matsushita cells and hence their data are not shown. The results shown are an average of data from two cells from

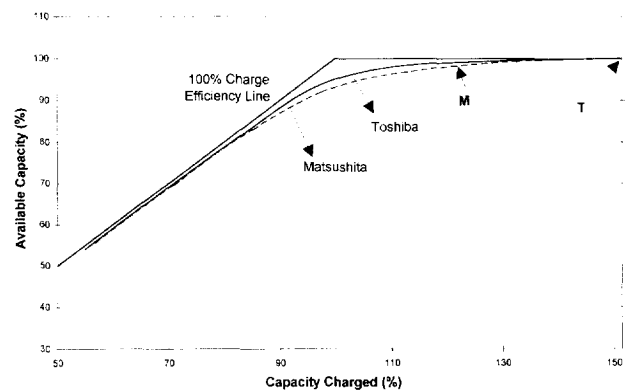


Fig. 4. Charge efficiency of the Matsushita and Toshiba cells at various inputs of charge. The available capacity or the charge efficiency deviates from the 100% efficiency line after about 90% charge input due to the onset of the recombination reaction. Points M and T refer to the recommended amounts of charge by the manufacturer for the Matsushita and Toshiba cells, respectively.

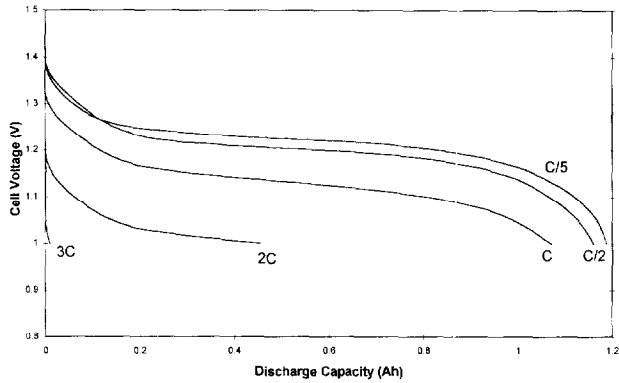


Fig. 5. Discharge characteristics of the Sanyo cell at various discharge rates. The cells were not discharged at 4C rate unlike the Toshiba and Matsushita cells due to their poor performance at 3C itself.

each manufacturer but there was no significant difference between each of the cells. However, a difference exists between the Toshiba and Matsushita cells as can be seen from the figure. Both of these cells require overcharge to attain 100% of the measured capacity shown in Table 1. From the charge efficiency curve, one can then identify the minimum charge that the battery needs on input to regain close to 100% of the rated capacity. It can be seen that after about 90% charge input, the slope of the efficiency curve decreases and we suspect that this is due to the recombination reaction.

The two points represented by M and T refer to the charge input as suggested by the product literature from Matsushita and Toshiba, respectively. This is shown in Table 2 as the suggested charge input in terms of the rated capacity. Although the discharge capacity does increase to a certain extent for both Matsushita and Toshiba after 100% of charge input, it still does not warrant the 150% charge input that is required for Toshiba Cells. It can be seen that the discharge capacity does not increase significantly between 120 and 150% charge input for the Toshiba cells and thus the charging protocol appears to be excessive. However, the Matsushita charging rationale appears

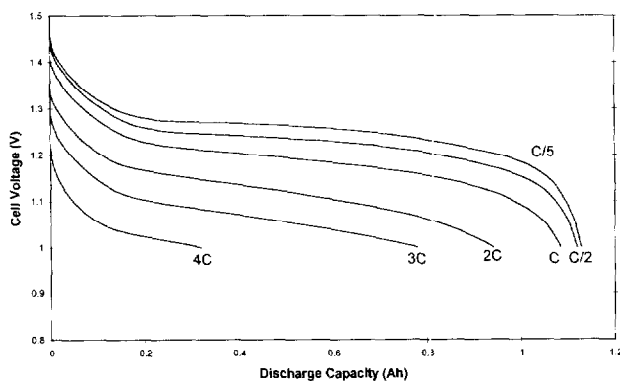


Fig. 6. Discharge characteristics of the Toshiba cell at various discharge rates. Although the Toshiba cells in general showed good high rate discharge capability, their performance fell slightly below than that claimed in their product literature.

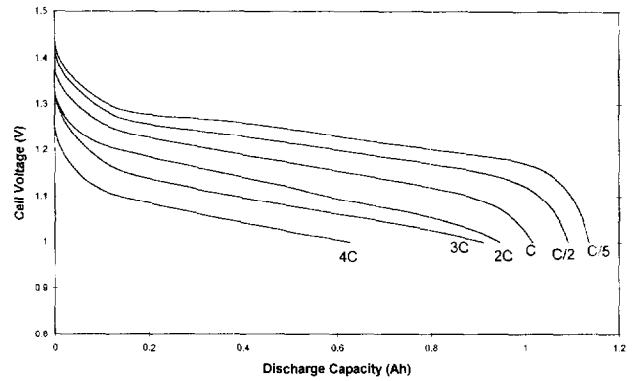


Fig. 7. Discharge characteristics of the Matsushita cell at various discharge rates. The Matsushita cells displayed superior characteristics at all rates of discharge and exhibited the performance claimed in their product literature.

to be valid. The cells were also charged at various rates (0.1C, 0.5C, and 1C) and charge acceptance was studied under these conditions. It was found that all the cells showed an increase in the charge acceptance with increase in the charge rate when the discharge rate was constant at 1C. The increase, although not very large, points to the fact why Matsushita does not suggest a low rate charging for their cells. Thus, all the cells were normally charged rapidly unless otherwise mentioned. It should be noted however that noted in all the cells, the increase in temperature during charge increased with the charging rate and this may be a disadvantage with applications that are sensitive to high temperatures.

3.3. Discharge rate capabilities

The cells were subjected to various discharge rates from C/5 to 4C to determine their performance over a range of conditions. Although continuous high rate discharges are not commonly found in most commercial applications, the results nevertheless show the flexibility of the cells. Fig. 5

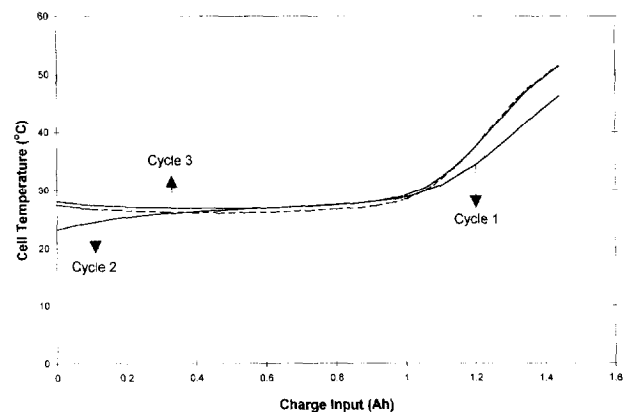


Fig. 8. Temperature profiles of a Matsushita cell during charge. This temperature increase which occurs due to the oxygen recombination reaction is comparable to all the cells and thus temperature profiles from other cells are not shown.

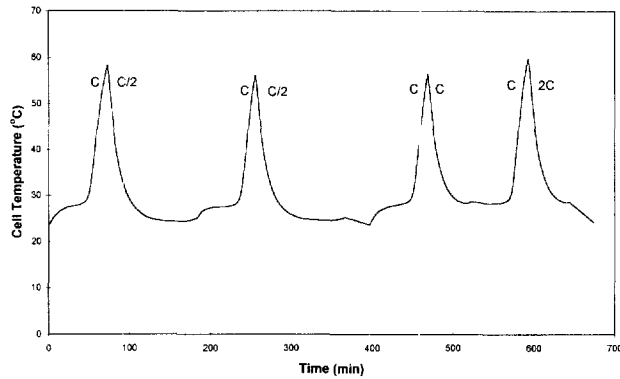


Fig. 9. Temperature profiles during charge and discharge in a Sanyo cell. The charging was kept constant at a C rate and the discharge rate was varied from C to $2C$. The temperature of the cell typically attains the ambient temperature at the end of discharge. There was no significant difference in the discharge capacity when there was a delay of 1 h between charge and discharge.

shows the discharge curves at various rates for the Sanyo cells. Albeit a minimum of four cells were utilized for these tests, performance of only the best cell is shown and the variation among the cells was less than 5% at the final capacity. It can be seen that there is a drastic reduction in the capacity for discharge rates over $1C$. The cell was thus not discharged at $4C$ unlike Toshiba and Matsushita cells. Figs. 6 and 7 show the discharge rate capabilities of Toshiba and Matsushita cells, respectively. The high rate performance of the Matsushita cells far surpasses the other two cells. The Matsushita cells were the only ones to give the performance cited in their product literature. The difference between the product literature and the performance was not apparent at low discharge rates for the Sanyo and the Toshiba cells.

Table 4

Comparison of the energy obtained from the various cells

Manufacturer	Energy (Wh)	No. of cells used in study	Energy density (Wh/kg)
Toshiba	1.53	6	60.5
Matsushita	1.48	8	57.4
Sanyo	1.47	6	57.4

3.4. Charge and discharge temperature characteristics

Fig. 8 shows the temperature change during charging of a Matsushita cell at $1C$ rate. The temperature starts to rise about 1 h after charging and this probably indicates the start of the recombination reaction. It can be further inferred that the maximum temperature increase occurs after one cycle. The maximum temperature which the cells from other manufacturers exhibited were very similar to each other. Fig. 9 shows the temperature profiles during charge and discharge at various discharge rates. The charging was constant at $1C$.

3.5. Discharge profiles for Sanyo and Matsushita cells

Fig. 10 shows the typical charge and discharge profiles for Sanyo and Matsushita cells. The behavior of the Toshiba cells was similar to the discharge profiles of the Sanyo cells and since their fast charging protocol is different from the other two cells, their profiles are not shown in this figure. It should be noticed that the discharge curves for the Sanyo cells exhibit a flat voltage behavior while the Matsushita cells show a continuous decrease in the voltage. Careful inspection of the discharge profiles for the

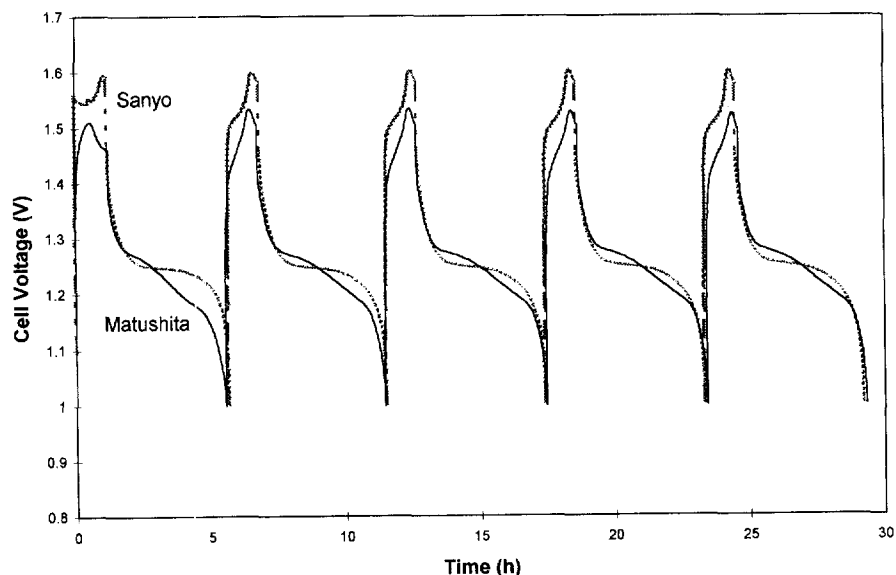


Fig. 10. Discharge profiles for Sanyo and Matsushita cells at $1C$ charge and $0.2C$ discharge. (Note the difference in the voltage profiles of the two cells, the Sanyo cell displaying a more flat voltage profile compared to the Matsushita cells.)

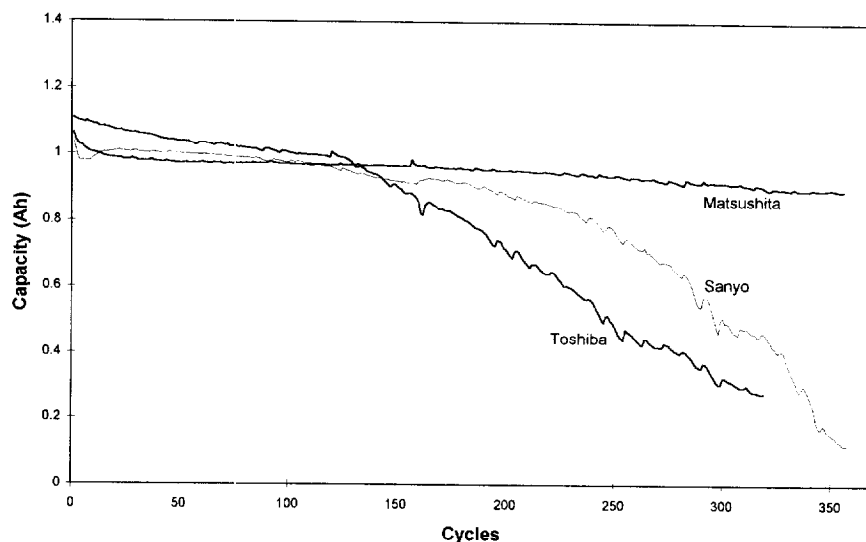


Fig. 11. Cycle-life studies of the three cells at 1C charge and discharge at room temperature. Although three cells from each manufacturer were used for the study, results from the cell which displayed the best characteristic are shown.

Matsushita cells reveals that there are two plateaus: one occurring at the very beginning of the discharge and the one occurring near the end of discharge.

3.6. Energy density

The energy density of the cells were calculated using the capacity obtained on $C/5$ discharge from all the cells. The capacity was measured until the cell potential reached 1.0 V. The energies are averages for the number of cells shown in Table 4. The energy density of the Toshiba cells were higher than that for the Sanyo and Matsushita cells which were comparable to each other as shown in Table 4. The cells were fast charged and subsequently discharged at a slower rate ($C/5$) to generate the maximum possible capacity. The Toshiba cells on an average exhibited higher capacities and when this is coupled with the flat discharge profiles, yield higher energy densities than the rest of the cells. It should however be noted that even though AA cells may not be optimized in terms of energy density and this may be the reason that the product literature from the various manufacturers does not report the energy density.

3.7. Cycle-life test

Three cells from each manufacturer were chosen for the cycle-life test. The cells were charged and discharged at a 1C rate. One hour of rest between charge and discharge was allowed for the temperature at the end of charging to decrease to the ambient temperature. Fig. 11 illustrates the behavior of the three cells on continuous charge/discharge. The graph shows the results from the cell which displayed the best behavior of the three cells from a manufacturer. Utmost there was a 20% decrease in the behavior between the cells from each manufacturer. The striking feature of the Matsushita cells lie in the fact that

there was very little variance in the behavior of the three cells. All the cells had approximately 90% of their initial capacity after 150 cycles. However, as the figure indicates, the capacity decayed at the fastest rate for the Toshiba cells. They reached 80% of their initial capacity after 150 cycles and the Sanyo cells reached 80% of their initial capacity in less than 200 cycles. The discharge capacity of the Matsushita cells remained flat with increase in the number of cycles and did not reach 80% of their initial capacity even after 375 cycles. Despite the fact that the Matsushita cells used the conventional polyamide separator, the loss of capacity with cycling, which has been considered to be a direct influence of the separator, is the least in these cells. This suggests that the cycle-life performance of the Matsushita cells might be further enhanced with a sulfonated polypropylene separator.

4. Conclusions

The characterization studies have illustrated the performance differences between three commercially available AA Ni/MH cell designs. Although the three brands were rated with identical capacity, weight, and other physical dimensions, their performance greatly differed in terms of charge and discharge behavior, high rate discharge capabilities, self-discharge, charging efficiency, and cycle life. Each manufacturer's cell had a certain good feature that was absent in the rest of the cells albeit the fact that the Matsushita cells stood out to be the best in terms of the overall performance. For instance, the Sanyo cells demonstrated a flat voltage profile during low rate discharge while the Matsushita cells had a markedly decreasing voltage profile. The Toshiba cells exhibited a slightly higher energy density and the lowest self-discharge rate. Matsushita cells exhibited little variance in terms of cycle

life and had superior high rate discharge capabilities and long cycle life. Despite the fact that the capacities of these cells were very similar, the charging protocols were dissimilar and the charge efficiency studies showed that the extensive overcharging specified by the Toshiba cells was not necessary. Most of the cells from each manufacturer under study exhibited fairly acceptable performance. The energy density may be improved with innovations in the area of developing high capacity metal-hydride electrodes because they currently account for 44% of the cell weight.

Acknowledgements

The authors gratefully acknowledge the financial support provided by the National Science Foundation Award

GER-9553409, an NSF/EPSCoR Industry Graduate Research Traineeship, and the Hoechst Celanese Corporation, Charlotte, NC. The authors also thank employees of the Hoechst Celanese Corporation: R.M. Spotnitz for his helpful discussions, Mark Ferebee for his laboratory assistance and Paige Good and Khuy Nguyen for their DSC analysis.

References

- [1] T.F. Fuller and J. Newman, *LBL Report, LBL-34390, UC-210*, 1993.
- [2] B.A. Johnson and R.E. White, Characterization of commercially available Li-ion batteries, *J. Power Sources*, accepted for publication.
- [3] M. Ikoma, Y. Hoshina, I. Matsumoto and C. Iwakura, *J. Electrochem. Soc.*, 143 (1996) 1904–1907.